Heliyon 5 (2019) e02887

Contents lists available at ScienceDirect

Heliyon

journal homepage: www.heliyon.com

Heliyon

Research article

A silver nanoparticle-poly(methyl methacrylate) based colorimetric sensor for the detection of hydrogen peroxide

Giorgio Giuseppe Carbone [a,*], Antonio Serra [b], Alessandro Buccolieri [a], Daniela Manno [b]

[a] Department of Biological and Environmental Sciences and Technologies (DiSTeBA), University of Salento, Via per Arnesano, 73100, Lecce, Italy
[b] Department of Mathematics and Physics "E. De Giorgi", University of Salento, Via per Arnesano, 73100, Lecce, Italy

ARTICLE INFO

Keywords:
Analytical chemistry
Materials science
LSPR
Silver nanoparticles
PMMA
TEM
Optical sensor
Hydrogen peroxide

ABSTRACT

A colorimetric sensor based on nanoparticles was developed for the detection of hydrogen peroxide. Nanoparticles were made using small sheets of poly(methyl methacrylate) (PMMA) and silver nitrate. The optical properties of the solution were characterized by spectrophotometer using the localized surface plasmon resonance (LSPR) phenomenon. The shape and size of the nanoparticles were obtained using a transmission electron microscope (TEM). Silver-poly(methyl methacrylate) nanoparticles solution (AgNP-PMMA) proved to be particularly sensitive to hydrogen peroxide compared to other analytes. This sensor provided a quick, practical and easy tool to detect hydrogen peroxide.

1. Introduction

Hydrogen peroxide (H_2O_2) is a very important compound involved in a great number of oxidative physiological processes [1, 2]. This molecule, the superoxide anion (O^{2-}) and the hydroxyl radical (•OH) are commonly known as free radicals and form a class of compounds called Reactive Oxygen Species (ROS).

A simple definition of free radicals was provided by Halliwell & Gutteridge, which defined them as molecules or molecular fragments containing one or more unpaired electrons in atomic or molecular orbitals [3]. This unpaired electron(s) usually gives an important degree of reactivity to the free radical.

A great part of the total ROS amount in our organism is produced in mitochondria as a result of the cellular respiration process [4]. In a healthy subject, it is estimated that the emission of ROS accounts for ~ 2% of the total oxygen spent by mitochondria [5]. Despite being very reactive, ROS produced by metabolism in physiological conditions are properly removed by our body. This process is called ROS homeostasis [6].

H_2O_2 is also a contaminant in many food [7], pharmaceutical [8] and environmental [9] processes. If this contaminant H_2O_2 is introduced into our organism, it cannot efficiently be removed by the ROS homeostasis process [10]. As a consequence, H_2O_2 excesses can lead to a pathological condition known as oxidative stress [11, 12], which can damage cellular lipids [13], proteins [14] or DNA [15].

In this context, the detection of H_2O_2 that contaminates commonly used substances represents an important target of clinical and industrial research. Classical methods for the detection of H_2O_2 such as fluorimetry [16] and titrimetry [17] have notorious drawbacks because they are time-consuming and expensive.

The advent of nanotechnologies has brought to alternative methods to sense H_2O_2, which take advantage from the unusual properties typical of the nanometric scale [18, 19]. These new methods allow reducing time analysis and costs considerably.

In recent years, the attention of the scientific community has been focusing in the use of silver nanoparticles (AgNP) to create sensors for hydrogen peroxide [20, 21] and in particular, AgNP for colorimetric sensors [22, 23]. In these devices, the analyte interaction with nanoparticles produces an absorbance variation that is proportional to its concentration. The phenomenon that causes this variation in absorbance is the Localized Surface Plasmon Resonance (LSPR). Nanoparticles are zero dimensional systems, in which electrons cannot freely move [24]. Therefore, electrons can be excited by a radiation of appropriate wavelength, giving rise to a collective oscillation known as Localized Surface Plasmon (LSP). These oscillations are closely related to the material of nanostructures, to their geometric properties (size, shape, density) and to the environment, in which they are immersed. In this way, a change in the solution in contact with the nanoparticles can be easily monitored,

* Corresponding author.
E-mail address: giorgiogiuseppe.carbone@unisalento.it (G.G. Carbone).

https://doi.org/10.1016/j.heliyon.2019.e02887
Received 15 April 2019; Received in revised form 5 September 2019; Accepted 15 November 2019

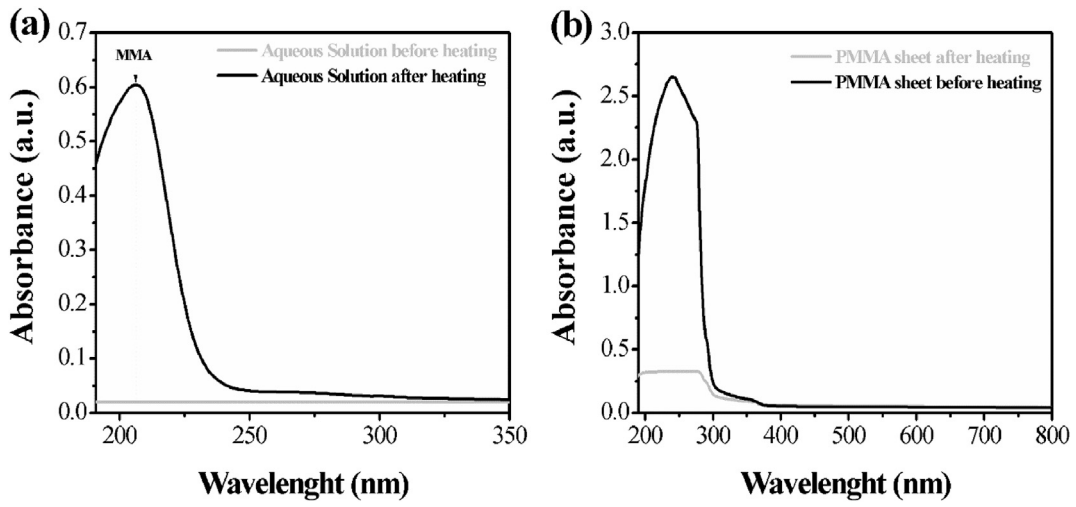

Fig. 1. UV-Vis spectra before and after the heat treatment of: a the aqueous solution containing the PMMA sheets; b the PMMA sheet.

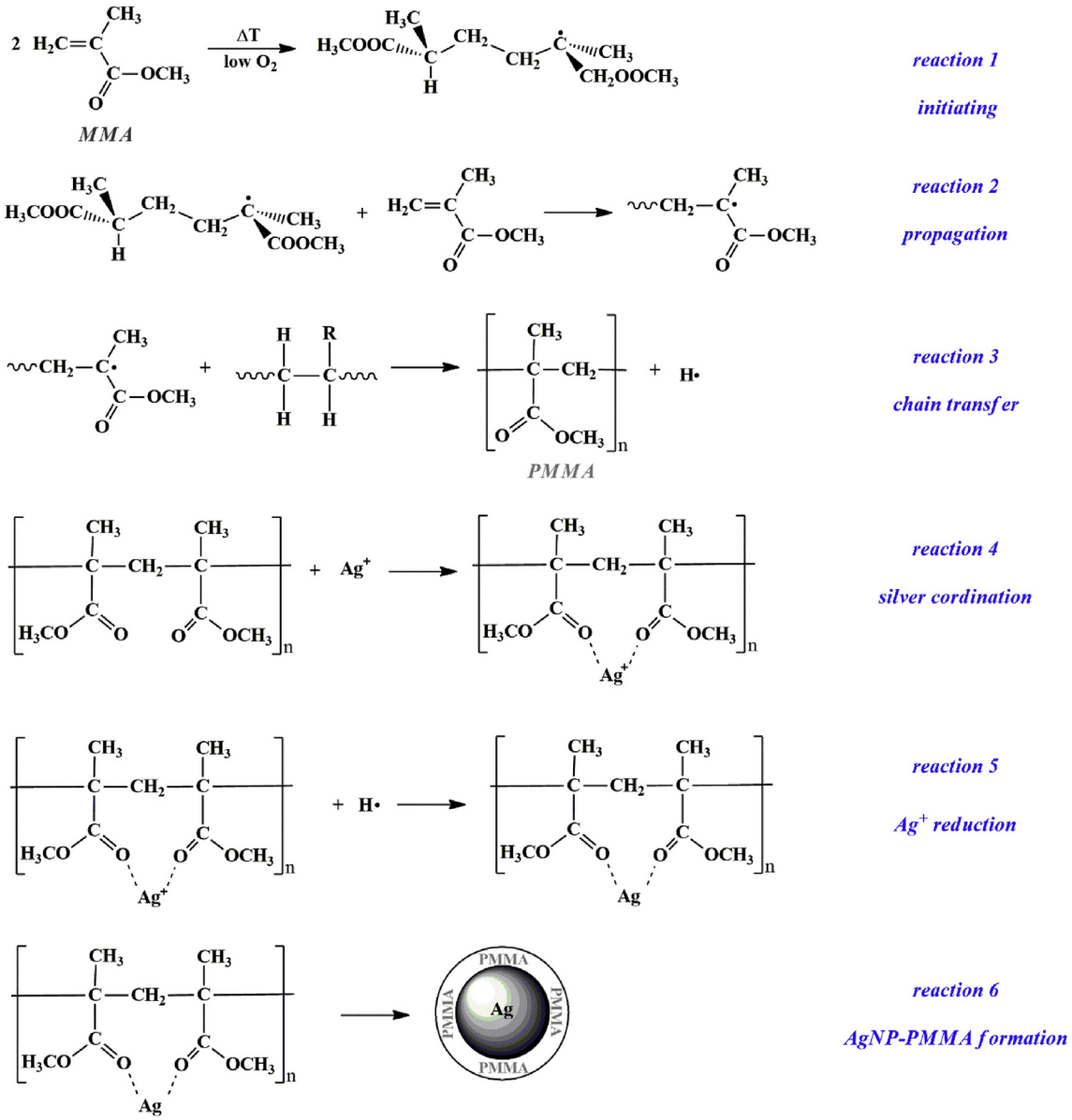

Scheme 1. Proposed mechanism for the formation of AgNP-PMMA during the spontaneous thermal polymerization of MMA.

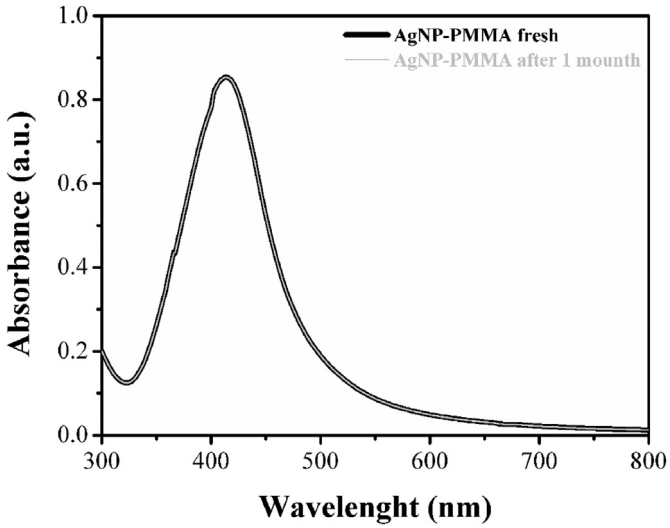

Fig. 2. UV-Vis spectra of AgNP-PMMA solution fresh and after one month.

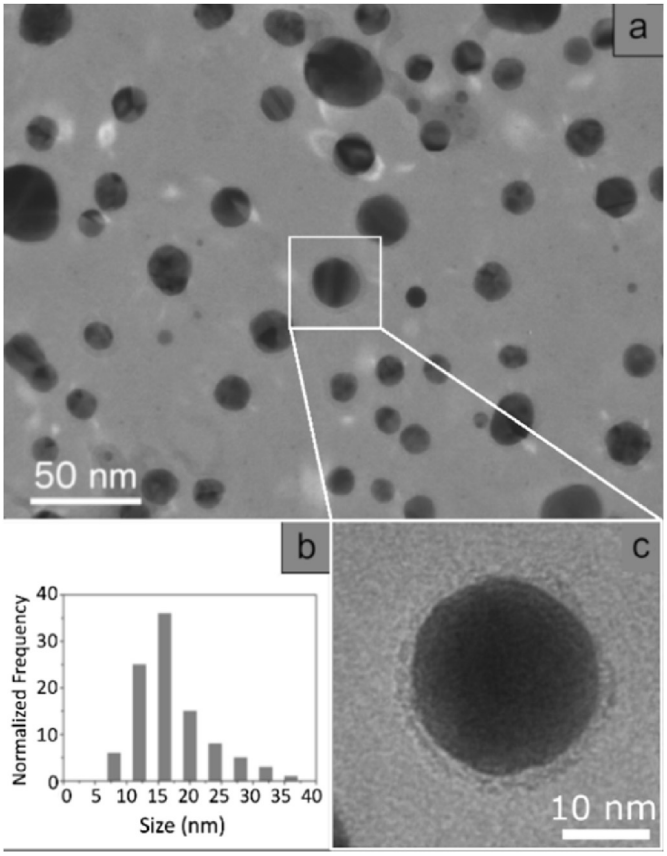

Fig. 3. (a) TEM image of the AgNP-PMMA colloidal solution; (b) Distribution size of AgNP-PMMA; c Enlargement of the nanoparticle in Fig. 3a.

inducing LSPR excitation with a spectrophotometer [25, 26].

Previous studies in literature showed LSPR based optical sensor, using polymer coated silver nanoparticles [27]. For example, Gavrilenko *et al.* showed the development of a colorimetric sensor based on silver nanoparticles embedded in a polymethacrylate matrix for the detection of hydrogen peroxide [28].

The aim of our work was the realization of a low-cost colorimetric sensor for H_2O_2 based on a colloidal solution of silver nanoparticles coated with poly(methyl methacrylate) (PMMA).

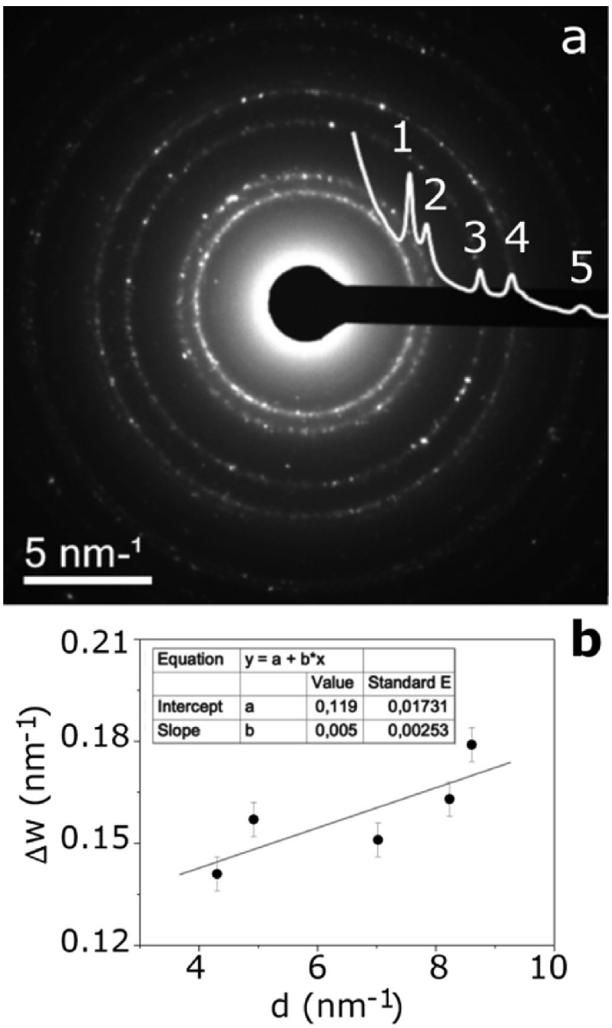

Fig. 4. (a) Diffraction ring showed by an AgNP-PMMA, (b) Williamson-Hall plot obtained from the electron diffraction profile.

PMMA is an amorphous polymer that belongs to the acrylate family. It owns very good optical properties [29] and a good degree of compatibility with human tissues [30]. Thanks to its high biocompatibility, PMMA is one of the most appreciated polymers for the realization of biomedical devices.

This polymer can also interact with metal nanoparticles, for example silver ones, improving their material properties. Among them, those that could be improved are mechanical strength, solubility and optical properties [31].

There are several attempts to synthetize silver nanoparticles embedded in PMMA. In these methods, silver ions are usually added to the polymer matrix and reduced to zero valent state by a heat treatment or by a reducing agent [32, 33, 34]. The substances that reduce silver ions in polymer matrix include toxic reagents like dimethylformamide (DMF), hydrazine and sodium borohydride [35, 36, 37].

In our work, we have obtained an aqueous colloidal solution of silver nanoparticles using PMMA as both capping and reducing agent. To the best of our knowledge there are no similar works reported in literature.

This study was conducted in two phases. In the first phase, silver nanoparticles coated with PMMA were synthetized by a method based on a thermal treatment of an aqueous solution containing small sheets of PMMA and silver nitrate. These nanoparticles were analyzed using UV–Vis spectrophotometry and transmission electron microscopy (TEM). In the second phase, it was realized a LSPR-based hydrogen peroxide sensor. The selectivity of the sensor was evaluated by testing other

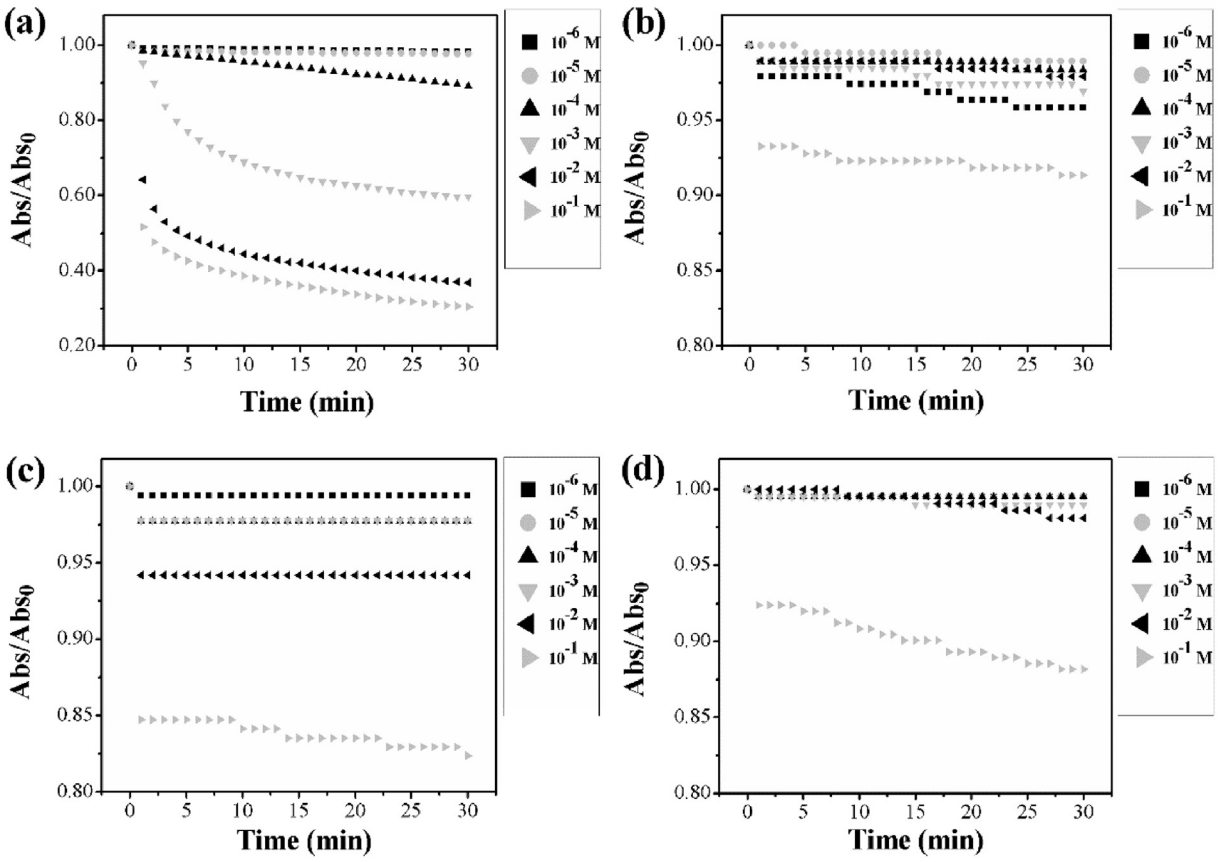

Fig. 5. Variation of the absorbance over time for different analytes: (a) hydrogen peroxide; (b) acetone; (c) ammonia; (d) ethanol.

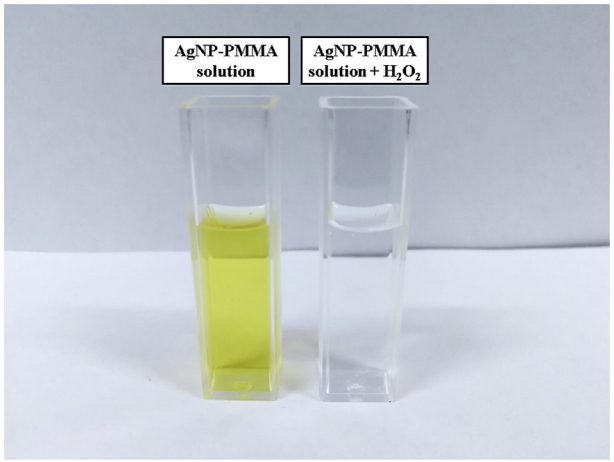

Fig. 6. AgNP–PMMA solution before and after adding H_2O_2.

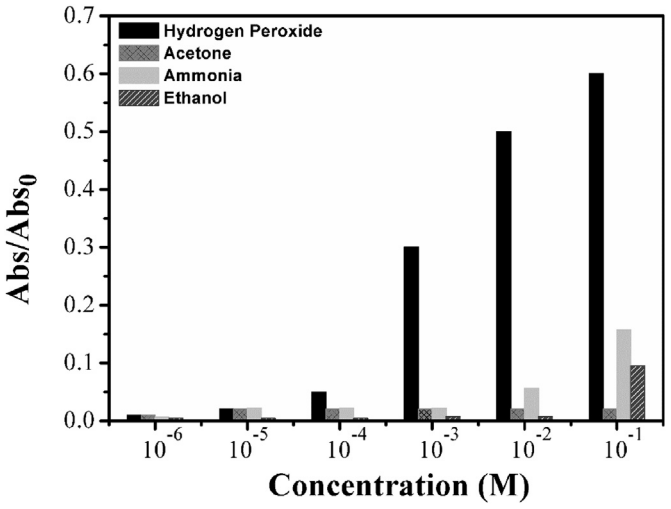

Fig. 7. Relationship between the average of absorbance values and the concentration for all investigated analytes.

molecules such as acetone, ethanol and ammonia.

2. Experimental

2.1. Materials

Silver nitrate ($AgNO_3$, 99 %) was purchased from Sigma Aldrich while PMMA sheets (sized to: w = 1 cm; h = 2,5 cm; thickness 0,07 cm) were purchased from GoodFellow (ME303004) and used for the synthesis of silver nanoparticles coated with poly(methyl methacrylate). Hydrogen peroxide 30 % (v/v), acetone 99 % (v/v), ethanol 99 % (v/v), ammonia 30 % (v/v) as analytes were purchased from Sigma-Aldrich.

Deionized water was obtained by a Zener Up 900 (Human Corporation) water purification system and used throughout the experiments. All PMMA sheets were washed by ultrasonication in ethanol for 3 min and then dried with a nitrogen spray gun prior to use.

Table 1
Comparison between the detection limit of our sensor and that of other jobs.

Authors	L.O.D [M]	Type of sensor
Our Work	10^{-6}	Optical
Moozarm Nia et al., 2015 [52]	$5{\cdot}10^{-5}$	Optical
Shu et al., 2007 [53]	10^{-6}	Optical
Lin et al., 2005 [54]	$7.6{\cdot}10^{-6}$	Optical
Cui, Kang et al., 2008 [55]	$1.7{\cdot}10^{-6}$	Electrochemical
Zhao et al., 2009 [56]	$1.2{\cdot}10^{-6}$	Electrochemical

2.2. Instruments

Ultraviolet–Visible spectroscopy. A UV/Vis spectrophotometer model T80 (Pg Instruments Ltd) was employed to study: a) the optical characteristics of the AgNP-PMMA colloidal solution by recording its absorbance in the range between 300 and 800 nm; b) the sensor response to different concentrations of various analytes. These measurements were carried out for each analyte by monitoring the absorbance variation with time (30 min) at 416 nm; c) the release of MMA monomers into the water solution used for the heat treatment of PMMA by measuring its absorption spectra in a range between 190 and 350 nm; d) the change in the optical characteristics of a PMMA sheet by recording its UV-Vis spectra before and after the thermal treatment.

Transmission Electron microscopy. TEM images and electron diffraction patterns were taken using an Hitachi 7700 transmission electron microscope operated at 100 kV. This acceleration voltage was settled to obtain a sufficient resolution and minimal radiation damage of the material. Specimens for TEM observations was prepared by drop-casting of freshly solutions containing Ag-PMMA nanoparticles onto standard carbon supported 600-mesh copper grid and drying slowly in air naturally.

2.3. Synthesis of silver nanoparticles coated with PMMA

In a typical synthesis, two PMMA sheets (0.6 g) are immerged into 10 mL of deionized water and heated to 90 °C for 1 h under magnetic stirring (SOL-A). The amount of PMMA has been optimized to obtain the largest amount of silver nanoparticles and to improve the stability of the solution over time.

An aqueous solution of silver nitrate (0.2 mM) was prepared and heated to 90 °C (SOL-B). After removing the PMMA sheets from SOL-A, 10 mL of SOL-B was added. The mixture was maintained at 90 °C for 1 h under vigorous stirring. In these conditions, the solution gradually changed from transparent to a pale yellow color.

3. Results and discussions

3.1. Formation of silver nanoparticles capped with PMMA

In the synthesis process of silver nanoparticles from $AgNO_3$, it is essential the reduction of Ag^+ to Ag^0. In order to meet this request, it is necessary the use of a reducing agent [38]. Excluding silver nitrate, we had only two compounds in our reaction mixture: PMMA and water. As regards water, it is well-known that it does not own enough reducing power to induce the formation of silver nanoparticles.

Thus, the only reagent in our solution that was able to reduce silver nitrate is PMMA. The question then arisen on how this was achieved. We supposed the involvement of methyl metacrylate (MMA) spontaneous thermal polymerization process in order to provide an explanation.

Before supplying a scheme on how this process could induce the formation of silver nanoparticles, it is necessary to give some clarifications. First, it will be described how the MMA becomes available in our solution and then how it can spontaneously polymerize in our reaction mixture.

MMA is the monomer that forms PMMA. It is well-known that PMMA presents residual monomers of MMA that have not joined in the formation of the polymer. Such monomers can be released by the PMMA if it is immersed in water for a certain period of time [39, 40, 41].

In order to verify that our PMMA sheets released MMA monomers in water, we analyzed the aqueous solution resulting from the heat treatment of PMMA with a spectrophotometer. The recorded spectrum (Fig. 1a) shows an absorption peak around 205 nm, which according to the studies of Lamb et al. is typical of MMA [42]. This experimental datum allowed us to assume that the heat treatment of PMMA with hot water induced a structural modification of the polymer, which facilitated the release of its residual MMA monomers.

In this respect, Devlin et al. showed that PMMA was capable of absorbing water molecules and that this phenomenon was much more evident when the water temperature is higher. This water absorption was responsible for the occurrence in the polymer of areas with different optical properties (plasticization) [43]. According to Devlin et al., the "plasticization" was due to the action of hot water by inducing molecular fragmentation and cavitation in the structure of the polymer.

By observing our PMMA sheets after the thermal treatment, we indeed noticed a plasticization-like effect. PMMA sheets appeared more opaque than the initial condition. This change in optical properties was also confirmed from the spectrophotometric analysis of PMMA sheets before and after the heat treatment. As shown in Fig. 1b, the thermal treatment make the PMMA more transparent to UV light. This left us to suppose that our PMMA sheets were also able to absorb water and as a result, the polymer altered its structural integrity.

In accordance with the studies of Devlin et al. about the water absorption by PMMA, we proceeded to weigh our PMMA sheets before and after the heat treatment. PMMA sheets showed an increase in weight of about 0.5% (from 0.6 g) that confirms the PMMA ability to absorb water.

All results confirmed that PMMA suffered structural integrity losses because of hot water treatment. Therefore, it was reasonable to think that this was the cause of the release in water of the MMA monomers contained in the polymer.

Realizing that PMMA could lose MMA in water, we should explain how these monomers could polymerize in our reaction mixture without the addition of any initiator. As it is known, the main reaction steps of this process are initiation, propagation and termination. Initiation consists in the formation of a radical from a monomer molecule so that it starts the polymerization process. Stickler et al. showed that MMA could spontaneously polymerize in this regard (Spontaneous Thermal Polymerization) [44]. They also proved that the conversion rate of MMA into PMMA was greater if the reaction environment had both a temperature around 100 °C and low oxygen levels. This condition also occurred in our reaction so we presumed that our MMA monomers spontaneous reacted to form a dimer-radical (Scheme 1, reaction 1).

Propagation is the reaction of a dimer-radical with a MMA molecule. This reaction allowed to increase the length of the polymer through the addition of the monomer, forming a macro-radical (Scheme 1, reaction 2). A reaction, which competes with propagation and takes place during MMA polymerization, is that of chain transfer. In this reaction, a radical might abstract a hydrogen atom from a polymer molecule. From this reaction, we could therefore assume that instantaneously a hydrogen radical was formed (Scheme 1, reaction 3).

As concerns silver, according to previous studies reported in literature [45, 46], the Ag^+ cations produced from the dissociation of $AgNO_3$ might coordinate with the oxygen atoms of PMMA (Scheme 1, reaction 4). Afterwards, Ag^+ was reduced to atomic silver by the hydrogen radicals formed from the chain transfer reaction (Scheme 1, reaction 5). Finally, silver produced aggregates to form Ag nanoparticles capped with PMMA (Scheme 1, reaction 6). The PMMA constituent prevented precipitation and further aggregation of AgNPs, while it stabilized and protected them through its carboxylate functional groups. The properties of the AgNP-PMMA were analyzed using UV–Vis spectrometry and TEM.

3.2. Optical and structural characterization of AgNP–PMMA solution

UV–Vis spectrophotometry was used to study the optical characteristics of the AgNP-PMMA solution because silver nanostructures with different shapes exhibited Localized Surface Plasmon Resonance (LSPR) bands at different frequencies [47]. In Fig. 2, a broad peak in the 350–500 nm spectral range is clearly visible with a maximum at 416 nm. This was due to surface SPR of electrons in the conduction bands of silver and indicated the formation of a colloidal solution with silver nanoparticles of nanometer-size dimensions.

We measured its absorption spectrum after one month, in order to test the solution stability. The spectrum remained unchanged as shown in Fig. 2, proving that PMMA prevented precipitation and further aggregation of silver nanoparticles.

The formation of silver nanoparticles was also confirmed by TEM image. The size, shape and morphology of the synthesized Ag nanoparticles were also characterized by TEM.

Fig. 3a shows a typical light field image obtained from the colloidal solution. Digitized TEM images were acquired from 20 randomly selected fields and processed with Digital Micrograph, a Gatan software, in order to determine the size of the nanoparticles. The distribution of the corresponding particle size is plotted in the histogram shown in Fig. 3b and, as evidenced, is not perfectly Gaussian. This event was due to the presence of large nanoparticles.

Finally, Fig. 3c shows an enlargement of a single nanoparticle. As one can see, the nanoparticle has a "crown" and is reasonable to think that it was due to PMMA capping.

The synthesized nanoparticles had an average size of 16 nm and a standard deviation of 8 nm. Furthermore, the nanoparticles had an isotropic morphology: they were approximately spherical. Electron diffraction patterns had pointed out the crystalline nature of the Ag nanoparticles. A typical selected-area electron diffraction (SAED) pattern, recorded on the areas shown in Fig. 3a, is presented in Fig. 4a and presents well-defined diffraction rings, a typical feature of random arrangement of nanocrystals. The diffraction profile superimposed to SAED pattern was obtained by software PASAD-tools through azimuthal integration. The line profile might be indexed, according to the fcc structure of Ag (JCPDS cards 4–0783) [Joint Committee for Powder Diffraction Standards, JCPDS, Card No. 04–0783]: the five peak (labeled 1, 2, 3, 4 and 5) correspond to (111), (200), (220), (311), and (222) allowed reflection respectively.

The peak broadening caused by reduced size of nanocrystals and residual strain can be interpreted according to Williamson-Hall model [48]. The theory, developed for X-ray diffraction, can be modified to electronic diffraction [49]:

$$\Delta \frac{1}{d_{hkl}} = \frac{2K}{D} + 4\varepsilon \frac{1}{d_{hkl}} \quad (1)$$

where $\Delta \frac{1}{d_{hkl}} = \Delta W$ is the amplitude at half height of the considered peak, D the nanocrystal mean diameter, K a parameter that is considered equal to 1 for spherical crystal, ε the strain and d_{hkl} the interplanar spacing of the lattice plane that gave rise to the considered peak.

Fig. 4b shows the modified Williamson-Hall plot obtained from the electron diffraction profile. ΔW determined by PASAD software was plotted as a function of d_{hkl}.

D and ε can be determined by the intercept and the slope of the straight line interpolating the experimental points. In our case D = (17 ± 2) nm and ε = (1.2 ± 0.5) $\cdot 10^{-3}$.

3.3. Evaluation of AgNP-PMMA solution as hydrogen peroxide sensor

We analyzed the response of the AgNP–PMMA solution to hydrogen peroxide, but also to other molecules, such as acetone, ammonia and ethanol, in order to test that it was more sensitive to H_2O_2.

Each test was conducted in the same way for each analyte. 1 mL of the AgNP-PMMA solution was put in different cuvettes and in each of them, it was added a different concentration of the same analyte from 10^{-6} to 10^{-1} M. The response of the AgNP-PMMA solution to each analyte was evaluated by monitoring the absorbance of the solution every minute for 30 min at a fixed wavelength of 416 nm. It was chosen this wavelength because it corresponded to the absorbance maximum of the AgNP-PMMA solution spectra. The absorbance values registered (Abs) was normalized dividing them for the absorbance value recorded before adding the analyte for each cuvette (Abs_0).

The change of normalized absorbance over time for all the analytes is reported in Fig. 5. As shown, the highest absorbance variation was registered for H_2O_2 at concentration higher or equal to 10^{-4} M. This event was due to the catalytic ability of silver that induces the decomposition of H_2O_2 by oxidizing itself to Ag^+ ions [50, 51].

This ability was visually verifiable for H_2O_2 with the change in the color of the solution from pale yellow to transparent (Fig. 6).

On the other hand, acetone, ammonia and ethanol showed a weak response only at the highest concentrations (10^{-1} M).

We also reported the average absorbance in relation to its concentration between 10^{-6} and 10^{-1} M, in order to appreciate more the sensor response for each analytes (Fig. 7).

The detection limit of the sensor realized in this work is 10-6 M. This result is appreciable as can be seen from the comparison with other works in the literature (Table 1).

4. Conclusion

In the present work, we proposed a simple method for the synthesis of AgNP-PMMA. We studied the formation of nanoparticles using UV-Vis spectrometer, measured nanoparticle size and their size distribution using TEM technique and confirmed the crystalline nature of formed nanoparticles using SAED patterns.

The Ag-PMMA nanoparticles were stable and did not show any aggregation even after one month. It was demonstrated that our silver-based sensor response increased with the increasing concentration of hydrogen peroxide. Therefore, the others analytes did not show an appreciable response except for higher concentration, proving that our optical sensor is more sensitive to H_2O_2.

Many measurements often use natural enzymes to sense hydrogen peroxide. However, these enzymic colorimetric methods became expensive when used for a large amount of samples [57]. In comparison, our colorimetric sensor can be realized through a simple chemical route and used as a simple and fast sensor that can be applied in medical and environmental field.

Declarations

Author contribution statement

Giorgio Giuseppe Carbone, Antonio Serra, Alessandro Buccolieri, Daniela Manno: Conceived and designed the experiments; Performed the experiments; Analyzed and interpreted the data; Contributed reagents, materials, analysis tools or data; Wrote the paper.

Funding statement

This research did not receive any specific grant from funding agencies in the public, commercial, or not-for-profit sectors.

Competing interest statement

The authors declare no conflict of interest.

Additional information

No additional information is available for this paper.

References

[1] K. Asada, Ascorbate peroxidase - a hydrogen peroxide-scavenging enzyme in plants, Physiol. Plant. 85 (1992) 235–241.

[2] H. Miura, J.J. Bosnjak, G. Ning, T. Saito, M. Miura, D.D. Gutterman, Role for hydrogen peroxide in flow-induced dilation of human coronary arterioles, Circ. Res 92 (2003) 31e–40.

[3] B. Halliwell, J.M.C. Gutteridge, Free Radicals in Biology and Medicine, Fifth Edit, 2015. New York.

[4] D.B. Zorov, M. Juhaszova, S.J. Sollott, Mitochondrial reactive oxygen species (ROS) and ROS-induced ROS release, Physiol. Rev. 94 (2014) 909–950.

[5] B. Chance, H. Sies, A. Boveris, Hydroperoxide metabolism in mammalian organs, Physiol. Rev. 59 (1979) 527–605.

[6] P.D. Ray, B.-W. Huang, Y. Tsuji, Reactive oxygen species (ROS) homeostasis and redox regulation in cellular signaling, Cell. Signal. 24 (2012) 981–990.

[7] R.A.B. Silva, R.H.O. Montes, E.M. Richter, R.A.A. Munoz, Rapid and selective determination of hydrogen peroxide residues in milk by batch injection analysis with amperometric detection, Food Chem. 133 (2012) 200–204.

[8] P. Gimeno, C. Bousquet, N. Lassu, A.-F. Maggio, C. Civade, C. Brenier, L. Lempereur, High-performance liquid chromatography method for the determination of hydrogen peroxide present or released in teeth bleaching kits and hair cosmetic products, J. Pharm. Biomed. Anal. 107 (2015) 386–393.

[9] R.C. Matos, J.J. Pedrotti, L. Angnes, Flow-injection system with enzyme reactor for differential amperometric determination of hydrogen peroxide in rainwater, Anal. Chim. Acta 441 (2001) 73–79.

[10] M. Valko, D. Leibfritz, J. Moncol, M.T.D. Cronin, M. Mazur, J. Telser, Free radicals and antioxidants in normal physiological functions and human disease, Int. J. Biochem. Cell Biol. 39 (2007) 44–84.

[11] R. Kohen, A. Nyska, Invited review: oxidation of biological systems: oxidative stress phenomena, antioxidants, redox reactions, and methods for their quantification, Toxicol. Pathol. 30 (2002) 620–650.

[12] B.E. Watt, A.T. Proudfoot, J.A. Vale, Hydrogen peroxide poisoning, Toxicol. Rev. 23 (2004) 51–57.

[13] R. Pamplona, Membrane phospholipids, lipoxidative damage and molecular integrity: a causal role in aging and longevity, Biochim. Biophys. Acta Bioenerg. 1777 (2008) 1249–1262.

[14] M. Chevion, E. Berenshtein, E.R. Stadtman, Human studies related to protein oxidation: protein carbonyl content as a marker of damage, Free Radic. Res. 33 (Suppl) (2000) S99–108. (Accessed 9 January 2019).

[15] M. Valko, M. Izakovic, M. Mazur, C.J. Rhodes, J. Telser, Role of oxygen radicals in DNA damage and cancer incidence, Mol. Cell. Biochem. 266 (2004) 37–56.

[16] M. Zhou, Z. Diwu, N. Panchuk-Voloshina, R.P. Haugland, A stable nonfluorescent derivative of resorufin for the fluorometric determination of trace hydrogen peroxide: applications in detecting the activity of phagocyte NADPH oxidase and other oxidases, Anal. Biochem. 253 (1997) 162–168.

[17] N.V. Klassen, D. Marchington, H.C.E. McGowan, H_2O_2 determination by the I_3-method and by $KMnO_4$ titration, Anal. Chem. 66 (1994) 2921–2925.

[18] A.S. Rad, A. Mirabi, E. Binaian, H. Tayebi, A review on glucose and hydrogen peroxide biosensor based on modified electrode included silver nanoparticles, Int. J. Electrochem. Sci. 6 (2011) 3671–3683.

[19] W. Chen, S. Cai, Q.-Q. Ren, W. Wen, Y.-D. Zhao, Recent advances in electrochemical sensing for hydrogen peroxide: a review, Analyst 137 (2012) 49–58.

[20] R. Narayanaswamy, O.S. Wolfbeis, Optical Sensors, Springer Berlin Heidelberg, Berlin, Heidelberg, 2004.

[21] A. Üzer, S. Durmazel, E. Erçağ, R. Apak, Determination of hydrogen peroxide and triacetone triperoxide (TATP) with a silver nanoparticles-based turn-on colorimetric sensor, Sens. Actuators B Chem. 247 (2017) 98–107.

[22] K. Farhadi, M. Forough, R. Molaei, S. Hajizadeh, A. Rafipour, Highly selective Hg^{2+} colorimetric sensor using green synthesized and unmodified silver nanoparticles, Sens. Actuators B Chem. 161 (2012) 880–885.

[23] S. Basiri, A. Mehdinia, A. Jabbari, A sensitive triple colorimetric sensor based on plasmonic response quenching of green synthesized silver nanoparticles for determination of Fe^{2+}, hydrogen peroxide, and glucose, Colloids Surfaces A Physicochem. Eng. Asp. 545 (2018) 138–146.

[24] G. Schmid, Nanoparticles, Wiley-VCH Verlag GmbH & Co. KGaA, Weinheim, Germany, 2010.

[25] E. Hutter, J.H. Fendler, Exploitation of localized surface plasmon resonance, Adv. Mater. 16 (2004) 1685–1706.

[26] K.A. Willets, R.P. Van Duyne, Localized surface plasmon resonance spectroscopy and sensing, Annu. Rev. Phys. Chem. 58 (2007) 267–297.

[27] E. Filippo, A. Serra, D. Manno, Poly(vinyl alcohol) capped silver nanoparticles as localized surface plasmon resonance-based hydrogen peroxide sensor, Sens. Actuators B Chem. 138 (2009) 625–630.

[28] N.A. Gavrilenko, N.V. Saranchina, M.A. Gavrilenko, Colorimetric sensor based on silver nanoparticle – embedded polymethacrylate matrix, Adv. Mater. Res. 1040 (2014) 923–927.

[29] C.A. Harper, E.M. Petrie, Plastics Materials and Processes, John Wiley & Sons, Inc., Hoboken, NJ, USA, 2003.

[30] J.F. Mano, R.A. Sousa, L.F. Boesel, N.M. Neves, R.L. Reis, Bioinert, biodegradable and injectable polymeric matrix composites for hard tissue replacement: state of the art and recent developments, Compos. Sci. Technol. 64 (2004) 789–817.

[31] U. Ali, K.J.B.A. Karim, N.A. Buang, A review of the properties and applications of poly (methyl methacrylate) (PMMA), Polym. Rev. 55 (2015) 678–705.

[32] N. Singh, P.K. Khanna, In situ synthesis of silver nano-particles in polymethylmethacrylate, Mater. Chem. Phys. 104 (2007) 367–372.

[33] Y. Deng, Y. Sun, P. Wang, D. Zhang, H. Ming, Q. Zhang, In situ synthesis and nonlinear optical properties of Ag nanocomposite polymer films, Phys. E Low-Dimensional Syst. Nanostructures. 40 (2008) 911–914.

[34] H. Kong, J. Jang, Antibacterial properties of novel poly(methyl methacrylate) nanofiber containing silver nanoparticles, Langmuir 24 (2008) 2051–2056.

[35] A. Gescher, Metabolism of N,N-dimethylformamide: key to the understanding of its toxicity, Chem. Res. Toxicol. 6 (1993) 245–251.

[36] S. Garrod, M.E. Bollard, A.W. Nicholls, S.C. Connor, J. Connelly, J.K. Nicholson, E. Holmes, Integrated metabonomic analysis of the multiorgan effects of hydrazine toxicity in the rat, Chem. Res. Toxicol. 18 (2005) 115–122.

[37] A. Panáček, L. Kvítek, R. Prucek, M. Kolář, R. Večeřová, N. Pizúrová, V.K. Sharma, T. Nevěčná, R. Zboril, Silver colloid nanoparticles: synthesis, characterization, and their antibacterial activity, J. Phys. Chem. B 110 (2006) 16248–16253.

[38] S. Prabhu, E.K. Poulose, Silver nanoparticles: mechanism of antimicrobial action, synthesis, medical applications, and toxicity effects, Int. Nano Lett. 2 (2012) 32.

[39] V.M. Miettinen, P.K. Vallittu, Release of residual methyl methacrylate into water from glass fibre-poly(methyl methacrylate) composite used in dentures, Biomaterials 18 (1997) 181–185.

[40] P. Pfeiffer, E.-U. Rosenbauer, Residual methyl methacrylate monomer, water sorption, and water solubility of hypoallergenic denture base materials, J. Prosthet. Dent 92 (2004) 72–78.

[41] G. Bayraktar, B. Guvener, C. Bural, Y. Uresin, Influence of polymerization method, curing process, and length of time of storage in water on the residual methyl methacrylate content in dental acrylic resins, J. Biomed. Mater. Res. B Appl. Biomater. 76B (2006) 340–345.

[42] D.J. Lamb, B. Ellis, D. Priestley, Loss into water of residual monomer from autopolymerizing dental acrylic resin, Biomaterials 3 (1982) 155–159.

[43] H. Devlin, P. Kaushik, The effect of water absorption on acrylic surface properties, J. Prosthodont. 14 (2005) 233–238.

[44] M. Stickler, G. Meyerhoff, Die thermische polymerisation von Methylmethacrylat, 1. Polymerisation in substanz, die makromol, Chemie 179 (1978) 2729–2745.

[45] M.Z. Kassaee, M. Mohammadkhani, A. Akhavan, R. Mohammadi, In situ formation of silver nanoparticles in PMMA via reduction of silver ions by butylated hydroxytoluene, Struct. Chem. 22 (2011) 11–15.

[46] M.N. Siddiqui, H.H. Redhwi, E. Vakalopoulou, I. Tsagkalias, M.D. Ioannidou, D.S. Achilias, Synthesis, characterization and reaction kinetics of PMMA/silver nanocomposites prepared via in situ radical polymerization, Eur. Polym. J. 72 (2015) 256–269.

[47] Y. Sun, Y. Yin, B.T. Mayers, T. Herricks, Y. Xia, Uniform silver nanowires synthesis by reducing $AgNO_3$ with ethylene glycol in the presence of seeds and poly(vinyl pyrrolidone), Chem. Mater. 14 (2002) 4736–4745.

[48] G. Williamson, W. Hall, X-ray line broadening from filed aluminium and wolfram, Acta Metall. 1 (1953) 22–31.

[49] A. Serra, D. Manno, A. Buccolieri, G.G. Carbone, L. Calcagnile, Photochromic properties in silver-doped titania nanoparticles, Mater. Res. Express 6 (2018), 036206.

[50] P. Vasileva, B. Donkova, I. Karadjova, C. Dushkin, Synthesis of starch-stabilized silver nanoparticles and their application as a surface plasmon resonance-based sensor of hydrogen peroxide, Colloids Surfaces A Physicochem. Eng. Asp. 382 (2011) 203–210.

[51] T. Endo, Y. Yanagida, T. Hatsuzawa, Quantitative determination of hydrogen peroxide using polymer coated Ag nanoparticles, Measurement 41 (2008) 1045–1052.

[52] P. Moozarm Nia, F. Lorestani, W.P. Meng, Y. Alias, A novel non-enzymatic H_2O_2 sensor based on polypyrrole nanofibers–silver nanoparticles decorated reduced graphene oxide nano composites, Appl. Surf. Sci. 332 (2015) 648–656.

[53] X. Shu, Y. Chen, H. Yuan, S. Gao, D. Xiao, H_2O_2 sensor based on the room-temperature phosphorescence of nano TiO_2/SiO_2 composite, Anal. Chem. 79 (2007) 3695–3702.

[54] M.S. Lin, H.J. Leu, A Fe_3O_4-based chemical sensor for cathodic determination of hydrogen peroxide, Electroanalysis 17 (2005) 2068–2073.

[55] K. Cui, Y. Song, Y. Yao, Z. Huang, L. Wang, A novel hydrogen peroxide sensor based on Ag nanoparticles electrodeposited on DNA-networks modified glassy carbon electrode, Electrochem. Commun. 10 (2008) 663–667.

[56] B. Zhao, Z. Liu, Z. Liu, G. Liu, Z. Li, J. Wang, X. Dong, Silver microspheres for application as hydrogen peroxide sensor, Electrochem. Commun. 11 (2009) 1707–1710.

[57] A.K. Bhargava, H. Lal, C.S. Pundir, Discrete analysis of serum uric acid with immobilized uricase and peroxidase, J. Biochem. Biophys. Methods 39 (1999) 125–136.